First space-based observations of formic acid (HCOOH): Atmospheric Chemistry Experiment austral spring 2004 and 2005 Southern Hemisphere tropical-mid-latitude upper tropospheric measurements

Curtis P. Rinsland,[1] Chris D. Boone,[2] Peter F. Bernath,[2] Emmanuel Mahieu,[3] Rodolphe Zander,[3] Gaëlle Dufour,[4] Cathy Clerbaux,[5] Solène Turquety,[5] Linda Chiou,[6] John C. McConnell,[7] Lori Neary,[7] and Jacek W. Kaminski[7]

[1] The first space-based measurements of upper tropospheric (110–300 hPa) formic acid (HCOOH) are reported from 0.02 cm^{-1} resolution Atmospheric Chemistry Experiment (ACE) Fourier transform spectrometer solar occultation measurements at 16°S–43°S latitude during late September to early October in 2004 and 2005. A maximum upper tropospheric HCOOH mixing ratio of 3.13 ± 0.02 ppbv (1 ppbv = 10^{-9} per unit volume), 1 sigma, at 10.5 km altitude was measured during 2004 at 29.97°S latitude and a lower maximum HCOOH mixing ratio of 2.03 ± 0.28 ppbv, at 9.5 km altitude was measured during 2005. Fire counts, back trajectories, and correlations of HCOOH mixing ratios with ACE simultaneous measurements of other fire products confirm the elevated HCOOH mixing ratios originated primarily from tropical fire emissions. A HCOOH emission factor relative to CO of 1.99 ± 1.34 g kg^{-1} during 2004 in upper tropospheric plumes is inferred from a comparison with lower mixing ratios measured during the same time period assuming HITRAN 2004 spectroscopic parameters. **Citation:** Rinsland, C. P., et al. (2006), First space-based observations of formic acid (HCOOH): Atmospheric Chemistry Experiment austral spring 2004 and 2005 Southern Hemisphere tropical-mid-latitude upper tropospheric measurements, *Geophys. Res. Lett.*, *33*, L23804, doi:10.1029/2006GL027128.

1. Introduction

[2] Formic acid (HCOOH) has been observed throughout the troposphere in liquid, aerosol, and vapor phases [*Keene and Galloway*, 1988; *Talbot et al.*, 1988; *Klare et al.*, 1999; *Arlander et al.*, 1990]. It is an important oxygenated volatile organic compound (OVOC) with major limitations recognized in the ability of models to reproduce simultaneous measurements of OVOC chemistry, particularly in the dry upper troposphere where OVOCs are a major source of HO_x (OH + HO_2) in the background troposphere [*Christian et al.*, 2004]. Identified HCOOH sources include biomass burning, biogenic emissions from vegetation and soils, secondary production from organic precursors, and emissions from motor vehicles [*Rinsland et al.*, 2004, and references therein]. Atmospheric HCOOH influences pH-dependent chemical reactions in clouds and is a major acidic component of rain [*Keene and Galloway*, 1988]. The abundance of OVOCs in biomass-burning plumes is similar to or exceeds those of non-methane hydrocarbons [*Koppmann et al.*, 2005]. Organic fire emissions from biomass burning account for 70–80% of OVOC emissions [*Christian et al.*, 2004].

[3] The HCOOH lifetime ranges from several hours in the boundary layer to a few weeks in the free troposphere with wet and dry deposition the primary sink, and reactions with OH of lesser importance [*Rinsland et al.*, 2004]. No model predictions exist that take into account the complex distribution of HCOOH sources and sinks and the dependence of the emissions on fuel type [*Christian et al.*, 2003]. A 3-D model assuming formic acid is produced only from biomass burning sources significantly underestimated average free tropospheric mixing ratios retrieved from ground-based solar spectra recorded at northern lower midlatitudes [*Rinsland et al.*, 2004].

[4] Atmospheric HCOOH has been measured with a variety of methods [*Christian et al.*, 2004; *Rinsland et al.*, 2004]. Remote sensing techniques use the HCOOH ν_6 vibrational band with a Q branch in an atmospheric window at 1105 cm^{-1}. It is the strongest HCOOH infrared feature, and has been measured over surface paths including urban conditions, in aircraft spectra, from balloon-borne solar spectra, and in ground-based solar spectra [*Rinsland et al.*, 2004]. Early spectroscopic HCOOH quantifications assuming room temperature laboratory absorption cross sections [*Hanst and Hanst*, 1993] have been replaced by analysis with line-by-line parameters [*Perrin et al.*, 1999] from the high resolution transmission (HITRAN) 2004 compilation [*Rothman et al.*, 2005].

[5] We report the first satellite HCOOH mixing ratios retrieved from high spectral resolution solar occultation spectra recorded in the subtropics to mid-latitudes of the southern hemisphere in the upper troposphere (110–300 hPa) during late September to mid-October 2004 and 2005. An improved correction for the interferences overlapping the HCOOH ν_6 band Q branch is applied as compared to the method described in a previous analysis of ground-based solar spectra [*Rinsland et al.*, 2004]. The

[1] NASA Langley Research Center, Hampton, Virginia, USA.
[2] Department of Chemistry, University of Waterloo, Waterloo, Ontario, Canada.
[3] Institute of Astrophysics and Geophysics, University of Liège, Liege, Belgium.
[4] Laboratoire de Météorologie Dynamique, Palaiseau, France.
[5] Service d'Aéronomie, Institut Pierre-Simon Laplace, Paris, France.
[6] Science Applications International Corporation, Hampton, Virginia, USA.
[7] Department of Earth and Atmospheric Science, York University, Toronto, Ontario, Canada.

HCOOH emission factor relative to CO has been derived by comparing plume measurements with lower measurements assumed as background observations. The same procedure was used to estimate emission factors of C_2H_6 and HCN relative to CO. The inferred emission factors are compared with previously reported values. Verification of a primary association of the emissions with (vegetative) fires is obtained from fire counts, back trajectory calculations, and comparison of HCOOH upper tropospheric mixing ratios with simultaneous measurements of other biomass burning products. ACE measurements sample the same regions during two years with differences in the upper tropospheric mixing ratio time series. No HCOOH retrievals were reported from ATMOS (Atmospheric Trace MOlecule Spectroscopy) measurements [*Irion et al.*, 2002].

2. Measurement Time Series

[6] The Atmospheric Chemistry Experiment (ACE) is a Canadian-led mission for atmospheric remote sensing launched on 12 August 2003 into a $74°$ inclined orbit at 650 km altitude by a NASA-supplied Pegasus XL rocket [*Bernath et al.*, 2005]. Three instruments with a shared field of view record high resolution atmospheric spectra taking advantage of the high precision of the solar occultation technique. An infrared Fourier transform spectrometer (FTS) records solar spectra below 150 km altitude at 0.02 cm^{-1} spectral resolution (maximum optical path difference of ± 25 cm) from 750 to 4400 cm^{-1}. Full resolution spectra are recorded in 2 s with an altitude spacing determined by the scan time, typically $3-4$ km, varying from 2 km for long high beta angle (angle between the satellite velocity vector and the vector of the Sun) occultations to 6 km for occultations with a beta angle to 6 km for zero beta angle occultations. The FTS has a circular field of view with 1.25 mrad diameter [*Boone et al.*, 2005] and is self-calibrating as linear response photovoltaic detectors are used and low Sun solar occultation spectra are divided by exo-atmospheric solar spectra from the same occultation. The ACE orbit yields solar occultation measurements ($85°N-85°S$ latitude). Additional instruments include imagers with optical filters at 0.525 and 1.02 μm.

[7] Measurements yield frequent measurements of middle and upper tropospheric pollution, and we focus on HCOOH Austral spring 2004 and 2005 measurements ($15°S-45°S$ latitude) during a dry season in the tropics (September$-$October), when seasonally high accumulation of pollutants occurs particularly over the South Atlantic Ocean between Brazil and southern Africa when widespread vegetative fires are common [*Fishman et al.*, 1991].

3. Analysis

[8] Routine ACE FTS science measurements began in February 2004. Profiles of volume mixing ratios with associated statistical uncertainties are retrieved for individual molecules from fits to multiple species in pre-selected microwindows over pre-specified altitude ranges with an algorithm that uses non-linear least squares spectral curve fitting [*Boone et al.*, 2005]. Temperature profiles are retrieved assuming a realistic CO_2 volume mixing ratio profile. Profile retrievals below 12 km altitude assume

Canadian Meteorological Centre (CMC) temperatures for the observation location. Spectroscopic parameters and absorption cross sections are based on HITRAN 2004 [*Rothman et al.*, 2005]. Analysis for HCOOH is from simultaneous fittings of 5 microwindows over altitudes from 5 to 18 km at the equator, with a latitude-dependent maximum altitude to approximate variations in tropopause height for the latitudes measured by ACE ($85°N-85°S$). The selected windows account for interferences overlapping the primary absorption feature of HCOOH, the ν_6 band Q branch at 1105 cm^{-1}. Interferences fitted in the simultaneous analysis were HDO, CH_3D, O_3 isotopologue 2 (i.e., $OO^{18}O$), CCl_2F_2, and CHF_2Cl. Microwindow locations and widths were 1105.15 cm^{-1} and 1.40 cm^{-1}; 2657.23 cm^{-1} and 0.55 cm^{-1}; 1158.55 cm^{-1} and 0.28 cm^{-1}; 1103.63 cm^{-1} and 0.30 cm^{-1}; and 1105.95 cm^{-1} and 0.30 cm^{-1}, respectively. The first microwindow contains the HCOOH Q-branch. The other microwindows contain information on molecules with interferences in the primary microwindow and are used to improve the results for them. ACE retrievals revealed an inconsistency between the O_3 intensities derived from HITRAN 2004 parameters [*Rothman et al.*, 2005] above 1800 cm^{-1} as compared to those obtained from the 10 μm region, with 10 μm retrievals providing O_3 profiles with better consistency with correlative measurements than those derived from fits to the microwindows above 1800 cm^{-1}. As O_3 has strong spectral features in the windows selected for the HCOOH analysis, we assumed the corrected version 2.2 ozone retrievals.

[9] Measurements for similar 2004 and 2005 time periods obtained at high beta angle between late September and early October are reported with more frequent measurements in 2005 than 2004 due to an increase in satellite-ground downlink because of the availability of additional ground stations. Mixing ratios of HCOOH are compared with simultaneous measurements of other species with elevated emissions from biomass burning. Windows, interferences fitted and altitude range for the analysis of CO, HCN, C_2H_6, C_2H_2 mixing ratios and 1.02 μm extinction are the same as reported previously [*Rinsland et al.*, 2005a], and the spectral window and analysis procedure for CH_3OH were described previously [*Dufour et al.*, 2006].

4. Results and Discussion

[10] Figure 1 illustrates molecule-by-molecule simulations and an ACE upper tropospheric spectrum for $1102-1107$ cm^{-1}. Each spectrum is normalized and offset vertically for clarity. The calculated transmission is shown for each important absorber after convolution of the computed transmission spectrum with the ACE instrument function. Simulation for individual molecules is based on the temperature profile and tangent altitude of the spectrum after an atmospheric ray tracing calculation. The simulations and the measured spectrum illustrate the complexity of the absorption and the high signal-to-noise of the measurements. The predicted HCOOH absorption is based on a reference profile from northern mid-latitude balloon-borne measurements after the *a priori* vertical profile was scaled by a multiplicative factor to produce absorption by the 1105-cm^{-1} Q branch similar to that in the measured spectrum. The overlapping absorption from several molecules
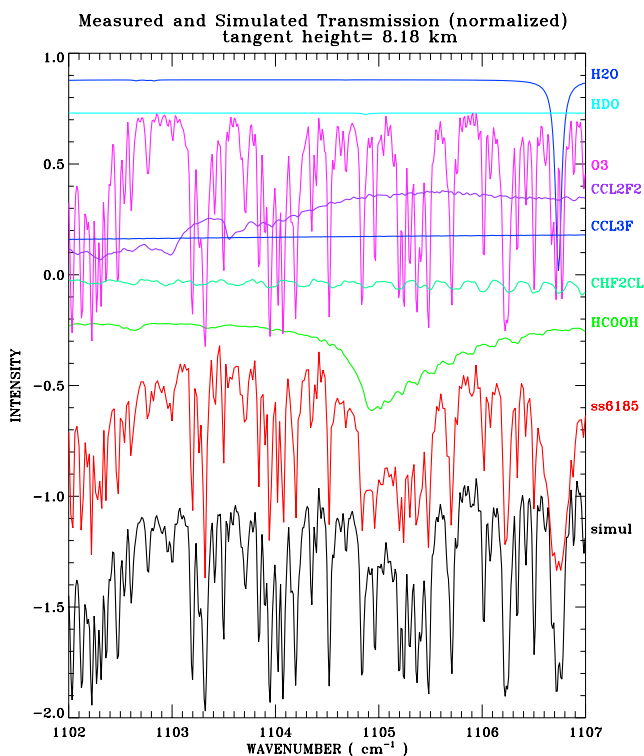
Figure 1. Comparison of molecule-by-molecule simulations of transmittance for the primary absorbers in the region containing the ν_6 band Q branch of HCOOH after transfer convolving the calculated monochromatic transmission with the ACE instrument line shape function. The black contour shows the calculation for all molecules (labeled simul), and an ACE solar spectrum (red). The simulations and measured spectra are normalized and offset vertically for clarity. The measured spectrum and its tangent height are identified. The occultation was recorded at 18.57°S latitude, 6.42°W longitude on 5 October 2004.

highlights the importance of a retrieval approach that accurately accounts for the attenuation by all interferences. Absorption by CH_4 and CO_2 are weaker than those shown in Figure 1, but both additional molecules are predicted to also contribute to the simulated spectrum above the noise level of ACE spectra. Additionally, HFC134a (CFH_2CF_3) has a Q-branch feature close to the HCOOH 1105-cm^{-1} Q branch absorption maximum. Although currently weak, HFC134a absorption is expected to increase with time, and its inclusion is planned in version 3 ACE results.

[11] There is an important difference in the simulations (Figure 1) as compared to those for ground-based solar spectra [e.g., *Rinsland et al.*, 2004, Figure 1]: absorption by HDO is predicted to be weaker in the upper troposphere than in ground-based solar spectra as a consequence of the general decline in the mixing ratio of H_2O and its isotopes with altitude. However, absorption by HDO cannot be neglected because of the close coincidence in the position of the ν_6 band Q branch and the high variability of HDO absorption. The HCOOH Q branch absorption depth in ground-based solar spectra is similar to that calculated for the HDO line at 1104.87594 cm^{-1} with a lower state energy of 701.6 cm^{-1} for background conditions [*Perrin*

et al., 1999]. Two weaker HDO lines at 1104.96910 and 1104.96941 cm^{-1} with intensities that have high sensitivity to temperature profile errors also overlap the HCOOH Q branch absorption. The bottom two plots show the transmission calculated for all gases along with the measured ACE spectrum. As a wide variation in absorption depth at the location of the HCOOH ν_6 band Q branch is observed in the ACE spectra, the improved procedure for retrieving the contributions of all significant interferences at each altitude was essential to yield reliable HCOOH profile retrievals.

[12] Figure 2 illustrates ACE tropospheric HCOOH, HCN, CO, C_2H_6, and 1.02 μm extinction at 110 to 300 hPa ($\sim$8– 16 km) for similar austral spring time periods in 2004 and 2005. The extinction at 1.02 μm was derived from averages of 3 pixels coincident with those from the FTS field of view. There is minimal extinction in cloud-free scenes at 1.02 μm except for aerosol and Rayleigh scattering. Objective criteria based on the measurement uncertainties were used to exclude noisy measurements from the time series.

[13] Correlation coefficients were derived from simultaneous measurements of HCOOH mixing ratios between $110-300$ hPa below the tropopause from National Center for Environmental Prediction (NCEP) measurements interpolated to ACE observation locations with those of C_2H_6, CO, C_2H_2, CH_3OH, CH_3Cl, SF_6, and 1.02 μm extinction per km from the 2004 and 2005 time series. High correlations between the trace gas mixing ratio and the 1.02 μm extinction coefficient per km with respect to CO were measured. Coefficients above 0.8 with respect to CO were obtained except for CH_3Cl-CO (0.55), CO-1.02 μm extinction (0.72), and CO-SF_6 (0.14). The SF_6 molecule was included to test of the validity of the procedure as only low emissions primarily from the flaming phase of biomass combustion have been reported [*Andreae and Merlet*, 2001, Table 1]. Emissions of SF_6 originate primarily from insulating electrical equipment releases [*Ko et al.*, 1993]. The high correlation coefficient of the well-established fire products with respect to CO confirms that fires were the dominant source of the emissions with lower mixing ratios also sampled (Figure 2), providing for a comparison of background and fire plume measurements, though as smoke ages, species within it are removed and others are generated by chemical and physical processes with a model required for further quantitative interpretation.

[14] Emissions of trace gases and aerosols from biomass burning have been reported in numerous studies with emission information that has been summarized for different emission sources, combustion processes, and emission stages [*Andreae and Merlet*, 2001]. Emission information is reported in two basic forms, emission ratios or emission factors for smoke constituents, and we report both for HCOOH relative to CO from ACE measurements from a comparison of profiles mixing ratios in plumes with measurements from occultations with low mixing ratios, which we assumed as representative of background conditions, as demonstrated in a study of CH_3OH upper tropospheric mixing ratios from ACE 2004 measurements [*Dufour et al.*, 2006, Figures 2 and 4]. The measurement of enhancements ("excess") mixing ratio relative to a background amount is a standard method with CO selected here as in many previous studies as the background reference. We use the 2004 time series for our study because of lower
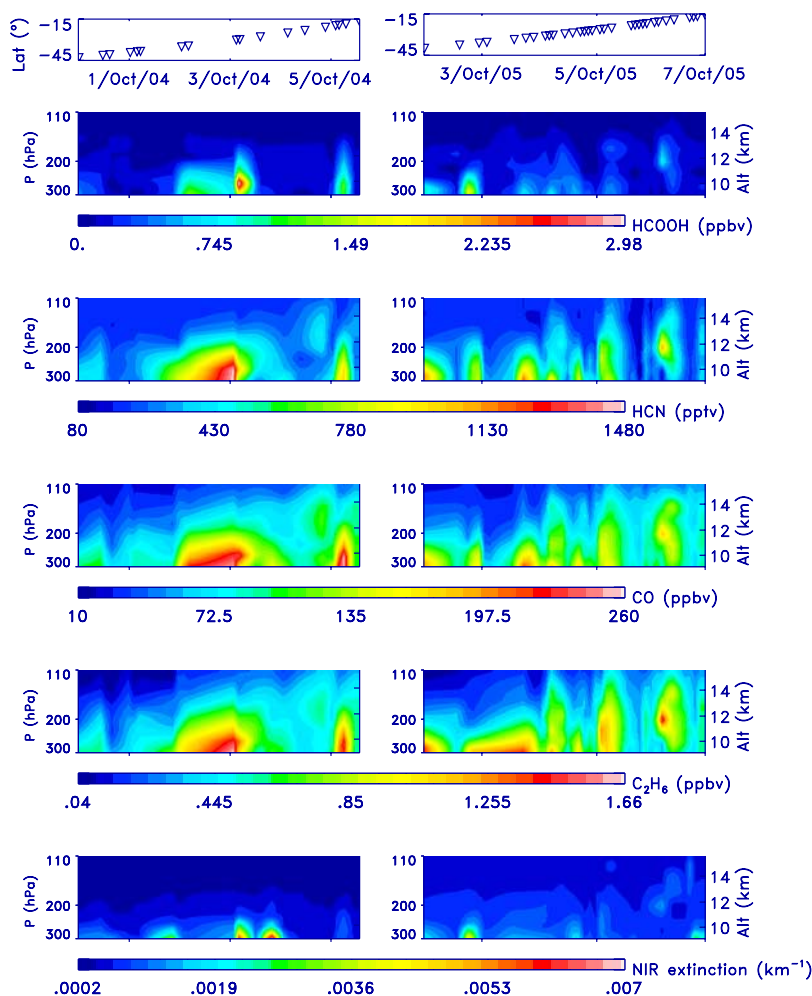
Figure 2. Austral spring time series of ACE upper tropospheric tropical and southern hemisphere mid-latitude occultation measurements of HCOOH, HCN, CO, C$_2$H$_6$, and 1.02 μm extinction from similar time periods in (left) 2004 and (right) 2005 vs. pressure. Inverted triangles at top indicate the latitude corresponding to the locations of individual measurements.

variability in HCOOH and other biomass burning products than during 2005 (see Figure 2).

[15] Measurements at 110–300 hPa below the tropopause were used to calculate mean CO, HCOOH, HCN, C$_2$H$_6$ mixing ratios for occultations between September 30 and October 6, 2004. Averages of these means were assumed for the background level of each molecule. Average background mixing ratios were 91.8 ppbv (from 17 profiles) for CO, 0.31 ppbv for HCOOH (from 14 profiles), 0.41 ppbv for HCN (from 16 profiles), and 0.57 ppbv for C$_2$H$_6$ (from 18 profiles). If the mixing ratio for each molecule exceeded the mean, the value was used to calculate the mean mixing ratio and the corresponding emission factor for that occultation assuming a CO emission factor of 107 g kg^{-1} for CO [*Andreae and Merlet*, 2001]. The HCOOH mixing ratio and 1-sigma uncertainties from 3 occultations with elevated mixing ratio are 0.94 ± 0.65 ppbv. Mixing ratios and standard deviations of CO from the same occultations are 140.5 ± 20.0 ppbv. We infer a HCOOH/CO 2004 emission ratio of 0.0114 ± 0.0076, corresponding to an emission factor of 1.99 ± 1.34 g kg^{-1}. Our results are consistent with the wide range of previously reported emission factors for forest fuels [*Andreae and Merlet*, 2001,

Table 1] with HCOOH/CO values of 0.13–2.9 g kg^{-1}. Recently, a HCOOH/CO emission ratio factor of 3.7 ± 2.1 g kg^{-1} was reported from the analysis of emissions of biomass from Australian mid-latitude forest fires [*Paton-Walsh et al.*, 2005, Table 3]. We analyzed the 2004 measurements with the same procedure to infer a C$_2$H$_6$/CO emission ratio of 0.0087 ± 0.0025 corresponding to an emission factor of 0.99 ± 0.29 g kg^{-1}, and a HCN/CO emission ratio of 0.0078±0.0044 corresponding to an emission factor of 0.80 ± 0.46 g kg^{-1}. Both results are consistent with results from previous fire emission studies [*Andreae and Merlet*, 2001, Table 1; *Paton-Walsh et al.*, 2005, Table 3].

[16] Figure 3 shows MODIS fire pixel counts (top) and kinematic back trajectories calculated with the HYSPLIT4 (Hybrid Single Particle Lagrangian Integrated Trajectory) model [*Draxler and Hess*, 1997] for 2 lower mid-latitude southern hemisphere 2004 occultations with elevated upper tropospheric HCOOH. The bottom panel shows the altitude of the back trajectory as a function of time. The elevated upper tropospheric HCOOH mixing ratios and the other emissions (Figure 2) originated from tropical fire emissions. This conclusion is consistent with elevated biomass burning
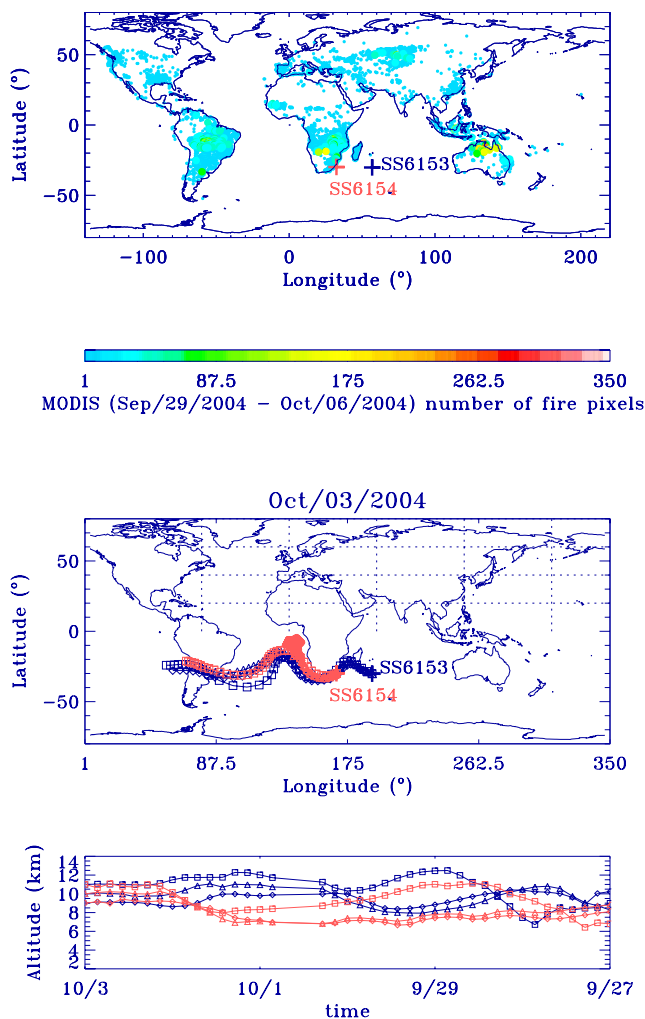
Figure 3. (top) Comparison of MODIS (Moderate Resolution Imaging Spectroradiometer) [*Giglio et al.*, 2003] fire pixel counts and back trajectory calculations for two lower mid-latitude southern hemisphere 2004 occultations with elevated upper tropospheric HCOOH at southern lower mid-latitudes. (bottom) Altitude of the back trajectory as a function of time.

products measured from high spectral resolution infrared solar spectra recorded at stations in New Zealand and Australia [*Rinsland et al.*, 2002], though HCOOH retrievals were not reported.

[17] Total uncertainty due to random errors at upper tropospheric altitudes is ~5%, resulting primarily from the statistical fitting uncertainty (~1%), errors in the pressure (~3%), and errors in the mixing ratios of molecules held fixed to the *a priori* profile (2−3% or less). Uncertainties in the ACE retrievals due to the absorbers overlapping the HCOOH 1105 cm^{-1} ν_6 band Q branch is included in the precision estimate. Primary source of systematic error is uncertainty in the spectroscopic parameters for HCOOH. The intensities of *Perrin et al.* [1999] have an accuracy of ±12% with the error reflecting the uncertainty in determining the partial pressures of the monomer with an uncertainty in its estimate due to dimer formation in the laboratory spectra. Measurements of the absolute intensity of the ν_6

band [*Vander Auwera et al.*, 2004; J. Vander Auwera, private communication, 2006] are a factor of two higher than those on HITRAN [*Rothman et al.*, 2005]. The *Perrin et al.* [1999] parameters assume all HCOOH lines have an air-broadening coefficient of 0.1 cm^{-1}atm^{-1} at 296 K with the temperature dependence coefficient n for air broadening set equal to 0.75. As the absorption by HCOOH is weak, sensitivity to errors in the air-broadening coefficient and its dependence with temperature are small. Based on these considerations, systematic error may be as high as a factor of two with the main error source the uncertainty in the absolute intensities due to possible bias in estimating the dimer contribution to the measured sample pressure. Systematic errors in mixing ratios due to differences in the retrieval algorithm are 5% or less based on comparisons of ACE profiles with those retrieved for the same events assuming ACE-derived temperatures and tangent heights with results obtained with an algorithm developed at the NASA Langley Research Center [*Rinsland et al.*, 2005b]. As optimal estimation is not used, retrievals from both are insensitive to the selection of the *a priori* mixing ratio profile. Temperature uncertainties in the troposphere and stratosphere are 2-3 K when compared to radiosonde measurement [*Kerzenmacher et al.*, 2005]. The contribution of temperature errors to HCOOH mixing ratio uncertainties is small to negligible.

5. Summary and Conclusions

[18] Time series of 0.02 cm^{-1} spectral resolution solar occultation spectra recorded during the Austral spring dry season of maximum biomass burning in 2004 and 2005 show elevated upper tropospheric HCOOH mixing ratios with maps of fire locations and back trajectory calculations indicating the elevated emissions originated from tropical regions where fires were frequent. High correlations of simultaneous HCOOH mixing ratios below the tropopause with those of well documented fire emission products confirm fires as the primarily source [*Fishman et al.*, 1991].

[19] A HCOOH emission ratio of 0.0113 ± 0.0076 relative to CO corresponding to an emission factor relative to CO of 1.99 ± 1.34 g kg^{-1} derived from a comparison of measurements in upper tropospheric plumes with occultations with low HCOOH mixing ratios assumed representative of background conditions is consistent with previously reported measurements of biomass burning emissions and inventories [*Andreae and Merlet*, 2001; *Paton-Walsh et al.*, 2005]. HITRAN 2004 spectral parameters [*Rothman et al.*, 2005] have been assumed.

[20] Our results demonstrate the potential for deriving HCOOH upper tropospheric mixing ratio distributions and biomass burning emission factors from satellite-borne infrared high resolution spectra. ACE measures simultaneous mixing ratios of HCOOH, HCN, CH$_3$OH, HCl, CH$_4$, C$_2$H$_4$, HCN, and HNO$_3$ includes major components of the HO$_x$ budget, in addition to O$_3$ in the upper troposphere. Measurements of HCOOH with the same infrared band and a similar window fitting procedure may be possible with other high spectral resolution satellite instruments.

References

Andreae, M. O., and P. Merlet (2001), Emissions of trace gases and aerosols from biomass burning, *Global Biogeochem. Cycles*, 15, 955–966.

Arlander, D. W., D. R. Cronn, J. C. Farmer, F. A. Menzia, and H. H. Westberg (1990), Gaseous oxygenated hydrocarbons in the remote marine troposphere, *J. Geophys. Res.*, 95, 16,391–16,403.

Bernath, P. F., et al. (2005), Atmospheric Chemistry Experiment (ACE): Mission overview, *Geophys. Res. Lett.*, 32, L15S01, doi:10.1029/2005GL022386.

Boone, C. D., et al. (2005), Retrievals for the Atmospheric Chemistry Experiment Fourier transform spectrometer, *Appl. Opt.*, 44, 7218–7231.

Christian, T. J., B. Kleiss, R. J. Yokelson, R. Holzinger, P. J. Crutzen, W. M. Hao, B. H. Saharjo, and D. E. Ward (2003), Comprehensive laboratory measurements of biomass-burning emissions: 1, Emissions from Indonesian, African, and other fuels, *J. Geophys. Res.*, 108(D23), 4719, doi:10.1029/2003JD003704.

Christian, T. J., B. Kleiss, R. J. Yokelson, R. Holzinger, P. J. Crutzen, W. M. Hao, T. Shirai, and D. R. Blake (2004), Comprehensive laboratory measurements of biomass-burning emissions: 2. First intercomparison of open-path FTIR, PTR-MS, and GC-MS/FID/ECD, *J. Geophys. Res.*, 109, D02311, doi:10.1029/2003JD003874.

Draxler, R. R., and G. D. Hess (1997), Description of the HYSPLIT_4 modeling system, *NOAA Tech. Memo. ERL ARL-224*, 27 pp., Natl. Tech. Inf. Serv., Springfield, Va.

Dufour, G., et al. (2006), First space-borne measurements of methanol inside aged tropical biomass burning plumes using the ACE-FTS, *Atmos. Chem. Phys. Dicuss.*, 6, 3945–3963.

Fishman, J. K., et al. (1991), Identification of widespread pollution in the Southern Hemisphere deduced from satellite analyses, *Science*, 252, 1693–1696.

Giglio, L., et al. (2003), An enhanced contextual fire detection algorithm from MODIS, *Remote Sens. Environ.*, 87, 272–283.

Hanst, P. L., and S. T. Hanst (1993), Database and Atlas: Infrared spectra for quantitative analysis of gases, Infrared Anal., Inc., Anaheim, Calif.

Irion, F. W., et al. (2002), The Atmospheric Trace Molecule Spectroscopy experiment (ATMOS) version 3 data retrievals, *Appl. Opt.*, 41, 6968–6979.

Keene, W. C., and J. N. Galloway (1988), The biogeochemical cycling of formic and acetic acids through the troposphere: An overview of current understanding, *Tellus, Ser. B*, 40, 322–344.

Kerzenmacher, T. E., et al. (2005), Measurements of O_3, NO_2 and temperature during the 2004 Canadian Arctic ACE validation campaign, *Geophys. Res. Lett.*, 32, L16S07, doi:10.1029/2005GL023032.

Klare, P., et al. (1999), Atmospheric formic and acetic acids: An overview, *Rev. Geophys.*, 37, 227–248.

Ko, M., et al. (1993), Atmospheric sulfur hexafluoride: Sources, sinks, and greenhouse warming, *J. Geophys. Res.*, 98, 10,499–10,507.

Koppmann, R., et al. (2005), A review of biomass burning emissions, part I: Gaseous emissions of carbon monoxide, methane, volatile organic compounds, and nitrogen-containing compounds, *Atmos. Chem. Phys. Discuss.*, 5, 10,455–10,516.

Paton-Walsh, C., N. B. Jones, S. R. Wilson, V. Haverd, A. Meier, D. W. T. Griffith, and C. P. Rinsland (2005), Measurements of trace gas emissions from Australian forest fires and correlations with coincident measurements of aerosol optical depth, *J. Geophys. Res.*, 110, D24305, doi:10.1029/2005JD006202.

Perrin, A., C. P. Rinsland, and A. Goldman (1999), Spectral parameters for the $\nu6$ region of HCOOH and its measurement in the infrared tropospheric spectrum, *J. Geophys. Res.*, 104, 18,661–18,666.

Rinsland, C. P., N. B. Jones, B. J. Connor, S. W. Wood, A. Goldman, T. M. Stephen, F. J. Murcray, L. S. Chiou, R. Zander, and E. Mahieu (2002), Multiyear infrared solar spectroscopic measurements of HCN, CO, C_2H_6, and C_2H_2 tropospheric columns above Lauder, New Zealand (45°S latitude), *J. Geophys. Res.*, 107(D14), 4185, doi:10.1029/2001JD001150.

Rinsland, C. P., E. Mahieu, R. Zander, A. Goldman, S. Wood, and L. Chiou (2004), Free tropospheric measurements of formic acid (HCOOH) from infrared ground-based solar absorption spectra: Retrieval approach, evidence for a seasonal cycle, and comparison with model calculations, *J. Geophys. Res.*, 109, D18308, doi:10.1029/2004JD004917.

Rinsland, C. P., G. Dufour, C. D. Boone, P. F. Bernath, and L. Chiou (2005a), Atmospheric Chemistry Experiment (ACE) measurements of elevated Southern Hemisphere upper tropospheric CO, C_2H_6, HCN, and C_2H_2 mixing ratios from biomass burning emissions and long-range transport, *Geophys. Res. Lett.*, 32, L20803, doi:10.1029/2005GL024214.

Rinsland, C. P., et al. (2005b), Comparison of profiles retrieved from measurements by the Atmospheric Chemistry Experiment (ACE): Tropospheric and stratospheric species, paper presented at 60th Ohio State University International Symposium on Molecular Spectroscopy, Columbus, Ohio, 21–24 June.

Rothman, L. S., et al. (2005), The HITRAN 2004 molecular spectroscopy database, *J. Quant. Spectrosc. Radiat. Transfer*, 96, 139–204.

Talbot, R. W., K. M. Beecher, R. C. Harriss, and W. R. Cofer III (1988), Atmospheric geochemistry of formic and acetic acids at a mid-latitude temperate site, *J. Geophys. Res.*, 93, 1638–1652.

Vander Auwera, J., et al. (2004), Absolute intensities in the ν_6 band of trans-formic acid, paper presented at 59th Ohio State University International Symposium on molecular spectroscopy, Columbus, Ohio, 21–25 June .

_____

P. F. Bernath and C. D. Boone, Department of Chemistry, University of Waterloo, Waterloo, ON, Canada N2L 3G1.

L. Chiou, Science Applications International Corporation, One Enterprise Parkway, Hampton, VA 23666, USA.

C. Clerbaux and S. Turquety, Service d'Aéronomie, IPSL, Paris F-75005, France.

G. Dufour, Laboratoire de Météorologie Dynamique, Palaiseau F-91128, France.

E. Mahieu and R. Zander, Institute of Astrophysics and Geophysics, University of Liège, Liège B-4000, Belgium.

J. C. McConnell, L. Neary, and J. W. Kaminski, Department of Earth and Atmospheric Science, York University, Toronto, ON, Canada M3J 1P3.

C. P. Rinsland, NASA Langley Research Center, Mail Stop 401A, Hampton, VA 23681-2199, USA. (c.p.rinsland@larc.nasa.gov)